Multilayer magnetostrictive structure based surface acoustic wave devices

Huan Zhou, Abdelkrim Talbi, Nicolas Tiercelin, Olivier Bou Matar

Applied Physics Letters

Multilayer magnetostrictive structure based surface acoustic wave devices

Cite as: Appl. Phys. Lett. **104**, 114101 (2014); https://doi.org/10.1063/1.4868530
Submitted: 06 January 2014 • Accepted: 25 February 2014 • Published Online: 17 March 2014

H. Zhou, A. Talbi, N. Tiercelin, et al.

Multilayer magnetostrictive structure based surface acoustic wave devices

H. Zhou, A. Talbi, N. Tiercelin, and O. Bou Matar[a)]
International Associated Laboratory LEMAC/LICS, IEMN UMR CNRS 8520, PRES Lille Nord de France, ECLille, 59652 Villeneuve d'Ascq, France

(Received 6 January 2014; accepted 25 February 2014; published online 17 March 2014)

This study addresses the experimental and theoretical investigations of guided elastic waves propagation in piezo-magnetic multi-layered structure. The structure is composed of a $20\times TbCo_{2(5nm)}/FeCo_{(5nm)}$ nanostructured multi-layer deposited between two Aluminum (Al) Inter-Digitals Transducers forming a surface acoustic wave delay line, on a Y-cut $LiNbO_3$ substrate. We compare the calculated and measured phase velocity variation under the action of the external magnetic field orientation and magnitude. We find quantitative agreement between the measured and modeled phase velocity shift for all external magnetic field configurations (hard axis and easy axis) and for different shape modes of elastic waves at their first and third harmonic operation frequencies. The shear horizontal mode exhibits a maximum phase velocity shift close to 20% for a ratio close to 1 between magneto-elastic film thickness and wavelength. © *2014 AIP Publishing LLC*. [http://dx.doi.org/10.1063/1.4868530]

Recent developments in physics and technology allow the elaboration of new magneto-electro-elastic materials such as multilayered piezoelectric-piezomagnetic composites.[1] Their large magnetoelectric coefficient, compared to one of the single phase materials, recently attracted a large number of studies,[2–4] and they are now widely used in the development of sensors, actuators, magnetic-electric energy converting devices, and solid state memories.[5–8]

High frequency Surface Acoustic Waves (SAW) propagation in piezoelectric- piezomagnetic composites, and particularly Rayleigh[9,10] or Love waves[11] in thin magnetostrictive films deposited on a piezoelectric substrate, has been studied long ago to develop tunable filters. There has recently been a renewed interest in this topic, due to the discovery that it is possible to drive spin pumping with SAW.[12] Most of these works have been made with magnetic material with low magnetostriction, such as Nickel, and/or without any indication regarding the magnetic state of the thin film. However, due to the magneto-elastic coupling, its elastic properties greatly depend on the magnetic state and on the applied magnetic field. It was also shown that in magnetoelastic films exhibiting in-plane uniaxial anisotropy, a high susceptibility to the external driving field can be obtained in the vicinity of a field-induced Spin Reorientation Transition (SRT).[13] To exploit these properties for RF applications, we investigate the propagation of SAW along the surface of piezoelectric substrate on which such a magnetostrictive thin film is deposited. We develop a theoretical description of the tunability of the SAW velocities, based on the derivation of an equivalent piezomagnetic material of a magnetostrictive thin film and use it in conjunction with a numerical method to compute propagation constants, i.e., dispersion curves, and mode shapes of elastic waves in layered piezoelectric-piezomagnetic composites deposited on a substrate.[14] This model can be used for different structures, such as composite membranes or films on a substrate, constituted of a large number of piezoelectric- piezomagnetic layers, and for an applied external magnetic field of any intensity and direction. Moreover, magnetization curves measured on real magnetic thin films can be introduced in calculations.

In this Letter, theoretical predictions are compared with the velocity variations, for both the Rayleigh and shear horizontal waves, measured in a sample realized in our laboratory: As shown on Fig. 1, a 300 μm wide and 200 nm thick $20\times TbCo_{2(5\,nm)}/FeCo_{(5\,nm)}$ nanostructured uni-axial thin film is deposited by RF-Sputtering on a Y-cut $LiNbO_3$ substrate between two interdigitized transducers (IDT) with 16 μm digits. SAWs propagate along the X axis, which is also the easy axis (EA) of the magnetic film. The frequency response of the signal transmitted between the two IDT, i.e., the S21 characteristic, measured with a network analyzer (Agilent 8753) after deposition of the $TbCo_2$/FeCo thin film, is displayed in Fig. 2. The first and third harmonics of the Rayleigh wave and of the first shear horizontal mode appear clearly on this electrical characteristic at 232, 696, 271, and 822 MHz, respectively. The magnetization of the nanostructured $TbCo_2$/FeCo thin film has been measured with a vibrating Sampling Magnetometer (VSM). Magnetization remains in the plane of the field and the results obtained along the

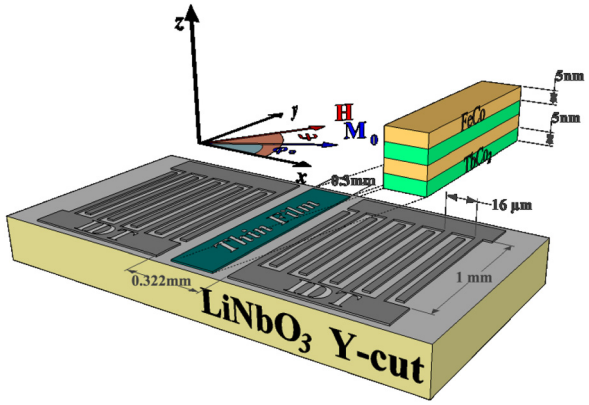

FIG. 1. Schematic description of the sample constituted of an uniaxial 200 nm $20\times TbCo_{2(5nm)}/FeCo_{(5nm)}$ nanostructured thin film deposited on a Y-cut $LiNbO_3$ substrate, and the associated coordinates system.

[a)]Electronic mail: olivier.boumatar@iemn.univ-lille1.fr

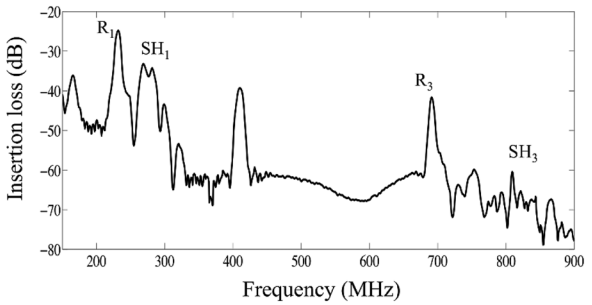

FIG. 2. Frequency response of the realized interdigitized transducer for surface acoustic wave on $LiNbO_3$ after deposition of the $TbCo_2$/FeCo thin film in the frequency range [150–900] MHz showing the first (R_1) and third harmonics (R_3) of the Rayleigh wave, and the first (SH_1) and third harmonics (SH_3) of shear horizontal mode.

easy and hard axis (HA) of the film are displayed in Fig. 3: they confirm the uni-axial anisotropy.

We consider a magneto-elastic wave in a ferromagnetic thin film deposited on a piezoelectric substrate and magnetized to saturation. In this case, the amplitude of the magnetization $\boldsymbol{M}$ is a constant M_s. The coupled equations for the mechanical and magnetic systems, i.e., the equations of motion and the Landau-Lifshitz equations, have the form[15]

$$\rho \frac{\partial^2 u_i}{\partial t^2} = \frac{\partial T_{ij}}{\partial x_j}, \tag{1}$$

$$\frac{\partial \boldsymbol{M}}{\partial t} = -\gamma \mu_0 [\boldsymbol{M} \times \boldsymbol{H}_{eff}], \tag{2}$$

where γ is the gyromagnetic ratio, u_i is the i^{th} component of the particle displacement, and x_i denotes the Eulerian coordinates. The effective internal magnetic field $\boldsymbol{H}_{eff}$ and the stress tensor T_{ij} are given by

$$\boldsymbol{H}_{eff} = \boldsymbol{H} - \frac{1}{\mu_0}\frac{\partial U}{\partial \boldsymbol{M}}, \tag{3}$$

$$T_{ij} = \frac{\partial U}{\partial E_{ij}}, \tag{4}$$

where $\boldsymbol{H}$ is the Maxwellian magnetic field, and E_{kl} is the strain tensor

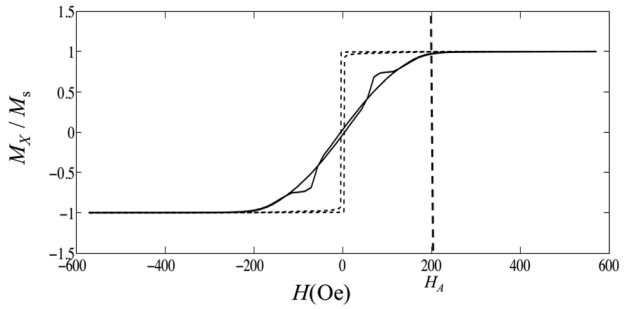

FIG. 3. Magnetization along the easy (dashed line) and hard axis (solid line) of the 200 nm nanostructured $TbCo_2$/FeCo thin film measured with a Vibrating Sample Magnetometer.

$$E_{kl} = \frac{1}{2}\left(\frac{\partial u_k}{\partial x_l} + \frac{\partial u_l}{\partial x_k}\right). \tag{5}$$

Here, U is the local internal energy density which can be written as the sum of a magnetic anisotropy, a magnetoelastic, and an elastic components. The magnetocrystalline anisotropy energy is given by $U_{an} = -K_1\alpha_1^2$, where $\alpha_1 = M_1/M_s$ are the direction cosines of $\boldsymbol{M}$ with respect to the induced EA (the Ox axis here). K_1 is the magnetic anisotropy constant linked to the anisotropy field H_A by $K_1 = \mu_0 M_s H_A/2$, where $\mu_0 = 4\pi 10^{-7}$ F/m is the magnetic permeability of vacuum. The magneto-elastic coupling energy has the form $U_{me} = b_{ijkl}\alpha_i\alpha_j E_{kl}$, where b_{ijkl} are the magneto-elastic constants and $\alpha_i = M_i/M_s$ are the direction cosines of $\boldsymbol{M}$ with respect to the chosen coordinates system. The elastic energy is given by $U_e = 1/2\ C_{ijkl}\ E_{ij}\ E_{kl}$, where C_{ijkl} are the second-order elastic constants. Linearizing the system of Eqs. (1) and (2) around a ground state position, which is dependent on the direction and intensity of the external applied magnetic field, we arrive at the piezomagnetic equations given by

$$\rho \frac{\partial^2 u_i}{\partial t^2} = \frac{\partial \sigma_{ij}}{\partial x_j}, \tag{6}$$

$$\frac{\partial b_i}{\partial x_i} = \frac{\partial\left(\mu_0(h_i + m_i)\right)}{\partial x_i} = 0, \tag{7}$$

with

$$\sigma_{ij} = \left(C_{ijkl} + \Delta C_{ijkl}\right)\frac{\partial u_k}{\partial x_l} - q_{lij}h_l, \tag{8}$$

$$b_i = q_{ikl}\frac{\partial u_k}{\partial x_l} + \mu_{il}h_l, \tag{9}$$

where the effective magnetic permeability and elastic constants are given by

$$\mu_{il} = \mu_0(\delta_{il} + \chi_{il}), \tag{10}$$

$$\Delta C_{ijkl} = b_{ijmn}\left(M_n^0 q_{mkl} + M_m^0 q_{nkl}\right). \tag{11}$$

The expressions of the piezomagnetic constants q_{ijk} and magnetic susceptibilities χ_{il} can be found in Ref. 16.

In the case of an uniaxial magnetostrictive thin film, supposed elastically and magneto-elastically isotropic, the magnetization is always in the plane of the film. Neglecting the influence of the static elastic strains, we obtain

$$\mu = \begin{bmatrix} \mu_{11} & \mu_{12} & 0 \\ \mu_{12} & \mu_{22} & 0 \\ 0 & 0 & \mu_{33} \end{bmatrix}, \tag{12}$$

$$\Delta C = \begin{bmatrix} \Delta C_{11} & \Delta C_{11} & 0 & 0 & 0 & \Delta C_{16} \\ \Delta C_{11} & \Delta C_{11} & 0 & 0 & 0 & -\Delta C_{16} \\ 0 & 0 & 0 & 0 & 0 & 0 \\ 0 & 0 & 0 & \Delta C_{44} & \Delta C_{45} & 0 \\ 0 & 0 & 0 & \Delta C_{45} & \Delta C_{55} & 0 \\ \Delta C_{16} & -\Delta C_{16} & 0 & 0 & 0 & \Delta C_{66} \end{bmatrix}, \tag{13}$$

TABLE I. Non zero components of the effective permeability tensor.

$$\mu_{11} = \mu_0 + \frac{\mu_0 M_s^2 \sin^2\varphi_0}{U'_{\varphi\varphi}}$$
$$\mu_{12} = -\frac{\mu_0 M_s^2 \sin 2\varphi_0}{2U'_{\varphi\varphi}}$$
$$\mu_{22} = \mu_0 + \frac{\mu_0 M_s^2}{U'_{\varphi\varphi}}\left(1 - \sin^2\varphi_0\right)$$
$$\mu_{33} = \mu_0 + \frac{\mu_0 M_s^2}{U'_{\theta\theta}}$$

$$q = \begin{bmatrix} q_{11} & -q_{11} & 0 & 0 & 0 & q_{16} \\ q_{21} & -q_{21} & 0 & 0 & 0 & q_{26} \\ 0 & 0 & 0 & q_{34} & q_{35} & 0 \end{bmatrix}, \qquad (14)$$

where the non zero components of the permeability, elastic stiffness corrections, and piezomagnetic constants tensors are given in Tables I, II and III, respectively. In these expressions, $b^{\gamma,2} = b_{1111}$ is the magneto-elastic coupling coefficient of the isotropic film, and

$$U'_{\theta\theta} = \mu_0 M_s(H_A(1 - \sin^2\varphi_0) + H\cos(\varphi_0 - \psi) + H_{me}),$$
$$U'_{\varphi\varphi} = \mu_0 M_s(H_A(1 - 2\sin^2\varphi_0) + H\cos(\varphi_0 - \psi) + H_{me}), \qquad (15)$$

where $H_{me} = (b^{\gamma,2})^2/(\mu_0 M_s C_{44})$ is the magneto-elastic field.

When the static external magnetic field is in the plane of the thin film, in a direction perpendicular to its EA, a phase transition, called SRT, appears at a field magnitude of H_A.[13] Under the SRT $\sin\varphi_0$ can be replaced by H/H_A in all the expression of the effective piezomagnetic constants. Above the SRT, $\sin\varphi_0 = 0$, and the effective constants of the equivalent piezomagnetic material simplify considerably. Some of the elastic constant variation expressions, ΔC_{11} and ΔC_{66}, have been derived by other authors[17] for a similar thin film configuration, using a less general method. Introducing the notation $h = H/H_A$, our expressions of ΔC_{66} and ΔC_{11} correspond perfectly to the shear modulus variation ($\Delta\gamma$) and the traction modulus variation ($\Delta\alpha$), respectively, obtained by these authors.

TABLE II. Non zero components of the effective elastic stiffness correction tensor.

$$\Delta C_{11} = -\frac{4(b^{\gamma,2})^2\cos^2\varphi_0\sin^2\varphi_0}{U'_{\varphi\varphi}}$$
$$\Delta C_{16} = \frac{(b^{\gamma,2})^2\sin 4\varphi_0}{2U'_{\varphi\varphi}}$$
$$\Delta C_{44} = -\frac{(b^{\gamma,2})^2\sin^2\varphi_0}{U'_{\theta\theta}}$$
$$\Delta C_{45} = -\frac{(b^{\gamma,2})^2\sin\varphi_0\cos\varphi_0}{U'_{\theta\theta}}$$
$$\Delta C_{55} = -\frac{(b^{\gamma,2})^2\cos^2\varphi_0}{U'_{\theta\theta}}$$
$$\Delta C_{66} = -\frac{(b^{\gamma,2})^2\cos^2 2\varphi_0}{U'_{\varphi\varphi}}$$

TABLE III. Non zero components of the effective piezomagnetic constant tensor.

$$q_{11} = -\frac{2b^{\gamma,2}\mu_0 M_s\cos\varphi_0\sin^2\varphi_0}{U'_{\varphi\varphi}}$$
$$q_{21} = \frac{2b^{\gamma,2}\mu_0 M_s\cos^2\varphi_0\sin\varphi_0}{U'_{\varphi\varphi}}$$
$$q_{34} = -\frac{b^{\gamma,2}\mu_0 M_s\sin\varphi_0}{U'_{\theta\theta}}$$
$$q_{35} = -\frac{b^{\gamma,2}\mu_0 M_s\cos\varphi_0}{U'_{\theta\theta}}$$
$$q_{16} = \frac{b^{\gamma,2}\mu_0 M_s\left(1-2\sin^2\varphi_0\right)\sin\varphi_0}{U'_{\varphi\varphi}}$$
$$q_{26} = -\frac{b^{\gamma,2}\mu_0 M_s\cos\varphi_0\left(1-2\sin^2\varphi_0\right)}{U'_{\varphi\varphi}}$$

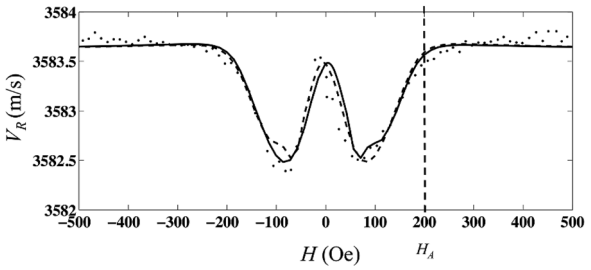

FIG. 4. Comparison between theoretical calculation (solid line) and experimental results (dots) for the variations of the Rayleigh wave's velocity as a function of the amplitude of a magnetic field applied along the hard axis.

The velocities of the two first modes of the sample, i.e., the Rayleigh wave and the first shear horizontal wave, have been measured as a function of the intensity of an external magnetic field applied along the hard axis of the magnetostrictive thin film. In Figs. 4 and 5, the experimental results (dots) are compared to the theoretical predictions obtained with the described effective piezomagnetic material model, in conjunction with a numerical Legendre/Laguerre polynomial expansion method to compute propagation constants and mode shapes of elastic waves in layered piezoelectric- piezomagnetic composites deposited on a substrate.[14] The considered elastic, magneto-elastic, and magnetic properties of the thin film are as follows: $C_{11} = 113.7$ GPa, $C_{44} = 31.3$ GPa, $b^{\gamma,2} = -8$ MPa, $M_s = 800$ kA/m, $H_A = 200$ Oe, $H_{me} = 20$ Oe. Except the elastic constants, taken from the literature, these properties have been measured in our laboratory.[2] The variation of the orientation of the magnetization, i.e., the angle φ_0, is determined from the magnetization curve displayed in Fig. 3. It is assumed that as the magnetic field decreases from a saturated state along the HA, the magnetization homogeneously rotates towards the EA in a "Stoner-Wohlfarth" fashion as it was discussed by Klimov *et al.*[18] The measured velocity variations of the first shear horizontal mode is 0.2%, which corresponds, as the film thickness is only 1.3% of the wavelength, to a variation of the elastic properties of the thin film of the order of 20%.

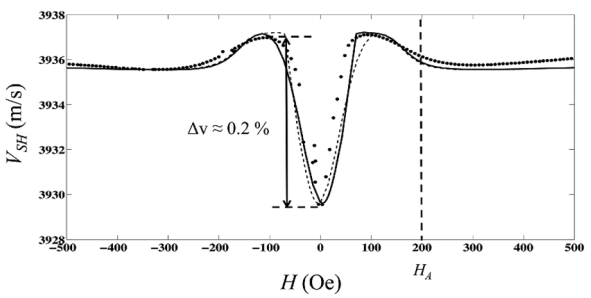

FIG. 5. Comparison between theoretical calculation (solid line) and experimental results (dots) for the variations of the first shear horizontal mode's velocity as a function of the amplitude of a magnetic field applied along the hard axis.

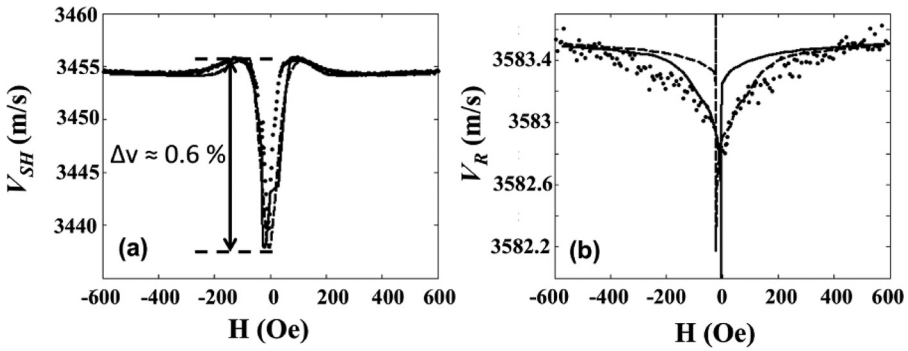

FIG. 6. Comparison between theoretical calculation (solid line) and experimental results (dots) for the variations of (a) the third shear horizontal mode's velocity as a function of the amplitude of an external magnetic field applied along the hard axis, and (b) the Rayleigh wave's velocity as a function of the amplitude of magnetic field applied along the EA.

The results obtained now for the variations of the third shear horizontal mode's velocity as a function of the amplitude of an external magnetic field applied along the hard axis, and of the Rayleigh wave's velocity for an external magnetic field applied along the EA, are displayed in Fig. 6. For the third shear horizontal mode, the velocity variations are three times the one measured for the fundamental mode, corresponding to the same 20% variation of the elastic constants. Moreover, the Rayleigh wave velocity variations are only 0.016% when the magnetic field is applied along the EA. This is 2.5 times less than the variations measured for the same mode when the magnetic field is applied along the hard axis, i.e., in the case of a SRT, demonstrating the importance of the magnetic state on these velocity variations as a function of the external magnetic field intensity.

In conclusion, we developed a theoretical model for the SAW velocity variations as a function of an external magnetic field in a thin film deposited on a piezoelectric substrate that is in good agreement with experimental results. The variations of the elastic properties in a magnetostrictive film can be huge and up to 20%. Optimized films with higher magnetoelastic coefficients $b^{\gamma,2}$ and a lower anisotropic field can further increase these variations. Magnetoelastic materials such as Metglas alloys are currently under investigation to develop a sensitive magnetic sensor using tunable magnetoacoustic phononic crystals.[19]

We acknowledge support from the French Agence Nationale de la Recherche Project 2010 BLAN 923-01.

[1]C. Nan, M. Bichurin, S. Dong, D. Viehland, and G. Srinivasan, J. Appl. Phys. **103**, 031101 (2008).
[2]N. Tiercelin, V. Preobrazhensky, P. Pernod, and A. Ostaschenko, Appl. Phys. Lett. **92**, 062904 (2008).
[3]N. Tiercelin, A. Talbi, V. Preobrazhensky, P. Pernod, V. Mortet, K. Haenen, and A. Soltani, Appl. Phys. Lett. **93**, 162902 (2008).
[4]A. Piorra, R. Jahns, I. Teliban, J. L. Gugat, M. Gerken, R. Knöchel, and E. Quandt, Appl. Phys. Lett. **103**, 032902 (2013).
[5]N. Spaldin and M. Fiebig, Science **309**, 391 (2005).
[6]N. Tiercelin, Y. Dusch, V. Preobrazhensky, and P. Pernod, J. Appl. Phys. **109**, 07D726 (2011).
[7]M. Weiler, L. Dreher, C. Heeg, H. Huebl, R. Gross, M. Brandt, and S. Groennenwein, Phys. Rev. Lett. **106**, 117601 (2011).
[8]B. Gojdka, R. Jahns, K. Meurisch, H. Greve, R. Adelung, E. Quandt, R. Knöchel, and F. Faupel, Appl. Phys. Lett. **99**, 223502 (2011).
[9]A. K. Ganguly, K. L. Davis, D. C. Webb, and C. Vittoria, J. Appl. Phys. **47**, 2696 (1976).
[10]R. F. Wiegert and M. Levy, Appl. Phys. Lett. **54**, 995 (1989).
[11]T. F. N. Yokokawa, S. Tanaka, and M. Inoue, J. Appl. Phys. **72**, 360 (1992).
[12]M. Weiler, H. Huebl, F. Goerg, F. Czeschka, R. Gross, and S. Groennenwein, Phys. Rev. Lett. **108**, 176601 (2012).
[13]N. Tiercelin, V. Preobrazhensky, P. Pernod, H. Le Gall, and J. BenYoussef, J. Magn. Magn. Mater. **210**, 302 (2000).
[14]O. Bou Matar, N. Gasmi, H. Zhou, M. Goueygou, and A. Talbi, J. Acoust. Soc. Am. **133**, 1415 (2013).
[15]A. Gurevich and G. Melkov, *Magnetization Oscillations and Waves* (CRC Press, Boca Raton, 1996).
[16]O. Bou Matar, J. Robillard, J. Vasseur, A.-C. Hladky-Hennion, P. Deymier, P. Pernod, and V. Preobrazhensky, J. Appl. Phys. **111**, 054901 (2012).
[17]Z. Sarkozi, K. Mackay, and J. Peuzin, J. Appl. Phys. **88**, 5827 (2000).
[18]A. Klimov, N. Tiercelin, V. Preobrazhensky, and P. Pernod, IEEE Trans. Magn. **42**, 3090 (2006).
[19]J.-F. Robillard, O. Bou Matar, J. O. Vasseur, P. A. Deymier, M. Stippinger, A.-C. Hladky-Hennion, Y. Pennec, and B. Djafari-Rouhani, Appl. Phys. Lett. **95**, 124104 (2009).